LAWRENCE
LIVERMORE
NATIONAL
LABORATORY

Real-structure effects: Band gaps of Mg_xZn_{1-x}O, Cd_xZn_{1-x}O, and n-type ZnO from ab-initio calculations

A. Schleife, F. Bechstedt

February 16, 2012

Disclaimer

This document was prepared as an account of work sponsored by an agency of the United States government. Neither the United States government nor Lawrence Livermore National Security, LLC, nor any of their employees makes any warranty, expressed or implied, or assumes any legal liability or responsibility for the accuracy, completeness, or usefulness of any information, apparatus, product, or process disclosed, or represents that its use would not infringe privately owned rights. Reference herein to any specific commercial product, process, or service by trade name, trademark, manufacturer, or otherwise does not necessarily constitute or imply its endorsement, recommendation, or favoring by the United States government or Lawrence Livermore National Security, LLC. The views and opinions of authors expressed herein do not necessarily state or reflect those of the United States government or Lawrence Livermore National Security, LLC, and shall not be used for advertising or product endorsement purposes.

Ab-initio description of quasiparticle band structures and optical near-edge absorption of transparent conducting oxides

André Schleife[1, 2, *] and Friedhelm Bechstedt[3, 2]

[1]*Condensed Matter and Materials Division,*

Lawrence Livermore National Laboratory, Livermore, California 94550, USA

[2]*European Theoretical Spectroscopy Facility (ETSF)*

[3]*Institut für Festkörpertheorie und -optik, Friedrich-Schiller-Universität,*

Max-Wien-Platz 1, 07743 Jena, Germany

(Dated: February 15, 2012)

Abstract

Many-body perturbation theory is applied to compute the quasiparticle electronic structures and the optical-absorption spectra (including excitonic effects) for several transparent conducting oxides. We discuss HSE+G_0W_0 results for band structures, fundamental band gaps, and effective electron masses of MgO, ZnO, CdO, SnO_2, SnO, In_2O_3, and SiO_2. The Bethe-Salpeter equation is solved to account for excitonic effects in the calculation of the frequency-dependent absorption coefficients. We show that the HSE+G_0W_0 approach and the solution of the Bethe-Salpeter equation are very well-suited to describe the electronic structure and the optical properties of various transparent conducting oxides in good agreement with experiment.

1

I. INTRODUCTION

Transparent conducting oxides (TCOs) combine high transparency in the visible spectral range with high electrical conductivity under ambient conditions.[1,2] Post-transition-metal compounds such as ZnO, In_2O_3, and SnO_2 are typical TCOs as they have large fundamental band gaps rendering these materials transparent into the ultraviolet (UV) spectral range. Due to their very large gaps, especially MgO and SiO_2 are transparent into the far UV. The gaps can be modified, e.g., by alloying ZnO with MgO or CdO (see Ref. 3 and references therein), but also by varying their chemistry, for instance when going from SnO_2 to SnO.[4] Free carriers, introduced by intentional as well as unintentional doping, are the reason for their remarkable conductivities.[5] Prominent examples are aluminum-doped ZnO,[6] tin-doped indium oxide,[7] antimony-doped SnO_2,[8,9] or even zinc-indium-tin oxide.[10]

Bulk TCO materials attract great attention due to their outstanding optical,[1] electrical,[11–13] and electrochemical[14] properties combined with excellent hardness and environmental stability.[1] This renders them highly interesting for applications as transparent front contacts for solar cells,[2,11,15,16] as next-generation gate oxides for Si-based electronics,[17] and in electrodes for photocatalytic water splitting.[18] Surfaces of the TCOs are highly interesting since for these an electron accumulation[19–21] as well as its depletion[22] have been observed. Exploring the atomic structure and the termination of surfaces of such oxides is still subject of current research.[23–25] In addition, the properties of the TCOs are drastically modified when they are prepared as nanobelts,[26] nanotubes,[27] nanoribbons,[28] nanowires,[29] and nanoparticles.[30]

Even though the TCOs are highly interesting for these reasons, their most desirable widespread application in semiconductor electronics, for instance as (light-emitting) diodes, is currently hampered by the lack of stable and reproducible *p*-type TCOs. For other photovoltaic or optoelectronic devices a deep understanding of intrinsic key properties is necessary. In this context, especially the electronic band structures around the fundamental gaps or the effective electron masses have to be thoroughly described. Also the optical-absorption properties near the band-edge and their dependence on the light polarization (due to dipole selection rules) need to be understood. For the TCOs a plethora of experimental results is available,[31,32] however, their interpretation can be challenging, for instance, due to sample-quality issues that depend on the manufacturing technique, the substrate temperature during growth, or the post-deposition treatment.[33] In the case of In_2O_3, growth can be phase selective and lead to both cubic as well as rhombohedral (*rh*) polymorphs

with band gaps differing by as much as 0.7 eV.[34] In the case of ZnO (see Ref. 35 and references therein), but also for SnO_2 (see Refs. 36–38 the details of the valence-band ordering and the band symmetries are not unequivocally determined from experiment.

Due to the continuous development of sophisticated methods and algorithms as well as the increasing power of today's supercomputers, the theoretical description of such material properties has made substantial progress during the last years. The accurate parameter-free description of the quasiparticle (QP) electronic structures and the frequency-dependent dielectric functions of complex materials (see the reviews in Refs. 39–42 and references therein) has become possible and leads – hand in hand with modern experimental techniques – to a deep understanding. Many-body perturbation theory is used to take the excitation aspect of important experimental techniques into account and can be applied to compute the electronic and spectral properties of bulk oxides in a given ideal crystal structure[43–46] but also for alloys,[3,47] oxide systems with defects,[48,49] and n-type TCOs.[50–52]

In Sec. II of the present paper we summarize the theoretical and computational approaches that we used to compute QP band structures and the optical absorption of various oxide materials. We present the corresponding band structures and provide detailed information about band gaps and effective masses in Sec. III. The line-shape and the oscillator strength of the optical absorption edges are discussed in Sec. IV. Section V summarizes this review paper.

II. THEORETICAL AND COMPUTATIONAL APPROACH

The present review paper focuses on the description of excited-state properties, such as the quasiparticle (QP) electronic structure and the optical absorption spectrum, for different oxides by means of an *ab-initio* framework. Their ground-state properties and, in particular, determining the equilibrium atomic geometries, e.g. within density-functional theory (DFT),[53,54] are not part of the present work. For more information about that as well as about all computational details we want to point the reader to Table I, which indicates the reference(s) in which the respective calculations are presented in more detail.

A. Quasiparticle electronic structures

Important experimental techniques such as (inverse) photoelectron spectroscopy or X-ray absorption and emission studies probe excited-state properties of a material, since during these processes an electron is added to or removed from the system. Hence, the ground-state description provided by a Kohn-Sham (KS) scheme within DFT is not sufficient, instead, QP effects have to be taken into account.[55] (Mis-) interpreting the KS eigenvalues[54] as excitation energies, typically leads to too small band gaps and wrong band dispersions,[55] since the KS eigenvalues neglect the excitation aspect that is characteristic for the experimental techniques that are used to measure these quantities.

Electronic excitations can accurately be treated by correctly describing the electronic self energy Σ. Expressing Σ as the product of the Green's function of the electrons G and the screened Coulomb potential W, as it was introduced by L. Hedin in 1965,[56,57] is an essential simplification of the description by neglecting vertex corrections. Nevertheless, the fully self-consistent solution of the resulting QP equation is very demanding from a computational point of view. For that reason it is common to rely on perturbation theory to compute QP energies in practice: In the G_0W_0 scheme first-order QP corrections are calculated for the eigenvalues of some starting electronic structure. It is immediately clear that any initial electronic structure must not be too far from the final results for first-order perturbation theory to be sufficient.

We found that the range-separated HSE06 hybrid functional,[58] but with a range-separation parameter of 0.15 a.u.$^{-1}$, as suggested by Paier *et al.*,[59,60] reasonably fulfills this requirement for several oxides.[43–45,61,62] In this work we review results for different TCOs that rely on the HSE functional to obtain the starting electronic structures for the G_0W_0 calculations; the entire approach is called HSE+G_0W_0 in the following. To keep the computational effort reasonable and since spin-orbit induced shifts are smaller than the QP corrections, we assume that the influence of the spin-orbit interaction on the QP corrections is negligible. Therefore, we take the spin-orbit interaction into account[63] only when calculating the HSE electronic structure and then apply the QP corrections calculated for spin-paired electrons.[62–64] Overall, we expect the QP energies calculated by the scheme outline above to be converged within about 0.1 eV.

A shortcoming of the HSE+G_0W_0 approach is its large computational cost. This becomes particularly problematic for the calculation of optical spectra, i.e., when significantly more **k**-points have to be taken into account for converging, for instance, the macroscopic dielectric function

around the absorption edge. In these cases we pursue a different approach by approximating the results of the HSE+G_0W_0 calculations via a DFT+U+Δ method,[3,41,43–45,61] where the term "DFT" indicates that either the local-density approximation (in the case of SnO_2 and SnO) or the generalized-gradient approximation (for MgO, ZnO, and CdO) is used. Therein, U, which denotes the additional Coulomb interaction term within the DFT+U approach,[65,66] is adjusted such that the energy position of the d bands matches the HSE+G_0W_0 result. In addition, Δ describes a scissors operator[67] that rigidly shifts all conduction bands so that the fundamental gap becomes identical to the HSE+G_0W_0 value.

The HSE+G_0W_0 as well as the DFT+U+Δ calculations are carried out using the Vienna Ab-Initio Simulation Package (VASP).[68–70] The wave functions are expanded into plane waves and the electron-ion interaction is described via the projector-augmented wave method.[71,72]

B. Optical absorption

In optical-absorption experiments excitation energies are studied that are not high enough to remove electrons from the system. Instead, upon the irradiation with light, an electron that gets excited from the valence bands into the conduction bands, leaves behind a hole in the valence bands. Due to their opposite charge, the photo-created hole and the excited electron interact via the screened Coulomb attraction, leading to the formation of excitons in the material. Excitonic effects due to the electron-hole interaction can, for instance, be taken into account in the *ab-initio* description by solving a Bethe-Salpeter equation (BSE) for the optical polarization function.[73,74]

For its numerical solution the BSE is typically rewritten into an eigenvalue problem for the electron-hole pair Hamiltonian.[74] We use the KS eigenstates from the DFT+U+Δ calculation to compute the matrix elements of the statically screened Coulomb attraction of the electrons and the holes as well as of the unscreened exchange-like term that accounts for local-field effects.[41,75] The DFT+U+Δ KS eigenvalues are used to describe the transition energies of non-interacting electrons and holes. The corresponding optical transition-matrix elements are computed using the longitudinal approximation.[76] After constructing the excitonic Hamiltonian, its eigenstates and eigenvalues can be used to calculate the optical properties of the system.[77–79]

The converged calculation of the optical absorption spectrum in the vicinity of the band edge requires a large number of $\mathbf{k}$ points.[43,80] Since for some of the materials discussed in this work the lowest optical transitions are confined to the vicinity of the Γ point, this part of the Brillouin zone

(BZ) can be sampled more densely to obtain convergence for the absorption edge;[80] we employ hybrid **k**-point meshes[80] to achieve that goal. However, the computational cost of diagonalizing the resulting excitonic Hamiltonian matrices with ranks N of up to $\approx 100{,}000$ is much too high. Therefore, in this work an efficient time-evolution scheme[81] is employed to calculate the dielectric function $\varepsilon(\omega)$ from the excitonic Hamiltonian.

When very dense **k**-point meshes are used, the large computational cost prohibits taking enough conduction bands into account for including high-energy optical transitions. This, however, becomes necessary to obtain converged results for the real part of $\varepsilon(\omega)$ at low photon energies due to the Kramers-Kronig relation[82] between the real and imaginary parts. Therefore, as described in detail in Refs. 43 and 45, we also solve a BSE using a more coarse **k**-point mesh to include optical transitions at intermediate energies. In addition, the optical transitions lying above this BSE cutoff are included (up to 200 eV) on the KS level. Finally, the absorption coefficient $\alpha(\omega)$ is calculated from the resulting dielectric function.

III. QUASIPARTICLE ELECTRONIC STRUCTURES

The QP band structures calculated using the HSE+G_0W_0 approach are depicted for MgO, ZnO, CdO, SnO_2, SnO, In_2O_3, and SiO_2 in Fig. 1. For the oxides studied in this work the uppermost valence bands are derived from O $2p$ states and the lowest conduction-band states originate from s states of the respective metal cation.[83]

In addition, from Fig. 1 it is obvious that MgO, ZnO, SnO_2, In_2O_3, and SiO_2 are direct semiconductors with the fundamental band gap at the Γ point; the two monoxides CdO and SnO are found to be indirect semiconductors. While in CdO the conduction-band minimum occurs at the Γ point and the maximum of the valence bands occurs away from Γ, the situation is different for SnO. In this material the valence-band maximum is located at Γ and the conduction band shows a pronounced minimum at the M point of the BZ, whereas Γ is an M_1 saddle point for the lowest conduction band (cf. Fig. 1). The direct and the indirect QP band gaps of these oxides are compiled in Table II. These results for the electronic structures have been carefully compared to experimental data[44,84–87] (see also Table I for the corresponding references) and the agreement is found to be rather good.

From Table II it also becomes clear that all the oxides studied in this work, with the exception of rocksalt- (*rs*) CdO and litharge- (*lt*) SnO, have fundamental band gaps that are large enough

for visible light not to be absorbed by the intrinsic materials. Even though the direct gaps at the Γ point are as large as 1.81 eV (*rs*-CdO) or even 3.21 eV (*lt*-SnO) the indirect gaps of these two materials are much smaller. Hence, phonon-assisted optical absorption can occur in the visible spectral range for samples of both materials. In addition, in the case of *lt*-SnO the smallest *direct* gap of only 2.68 eV occurs at the *M* point of the BZ.

The HSE+G_0W_0 results are used to derive the effective electron masses along different directions in the BZ via parabolic fitting to the QP band structures in the close vicinity of the Γ point (the *M* point in the case of SnO). We refer the reader to the literature for the effective masses that have been derived for the *rs* polymorphs of MgO and CdO,[45] *rt*-SnO$_2$,[44] *rh*-In$_2$O$_3$,[87] or the wurtzite (*wz*) polymorphs of MgO, ZnO, and CdO.[45,62] For beta-cristobalite- (β) SiO$_2$, effective electron masses of $m_L^*(\Gamma_{CBM})$=0.57, $m_K^*(\Gamma_{CBM})$=0.58, and $m_X^*(\Gamma_{CBM})$=0.57 are obtained and in the case of *lt*-SnO, the conduction-band minimum at the *M* point of the BZ leads to electron masses of $m_A^*(M_{CBM})$=0.37 and $m_\Gamma^*(M_{CBM})$=0.49 (all in units of the free-electron mass). We also use these values to derive the harmonic mean values of the electron masses for all the oxides (cf. Table II).

In the case of *rs*-MgO[45] we find a small anisotropy (indicating that the bands are not strictly parabolic within the **k** range used for the fit) and the two twofold degenerate valence bands are heavy-hole related (cf. Table III). Their masses are of the same order of magnitude in all three high-symmetry directions and are, roughly, one order of magnitude larger than the values for the light-hole band. Also the lowest CB turns out to be almost isotropic. As with *rs*-MgO, the two uppermost valence bands in *rs*-CdO are heavy-hole bands and the third one is of light-hole type.[45] Since for *rs*-CdO the valence-band maximum occurs away from the Γ point in the BZ, the values for the effective mass of the uppermost two valence bands are negative along certain directions in **k** space (cf. Table III). This has been traced back to the fact the the *pd* hybridization is forbidden at Γ due to the *rs* lattice symmetry.[45,88] In this material holes are expected to occur at the valence-band maximum between *K* and Γ. We observe that the effective electron masses for β-SiO$_2$ are very isotropic; the anisotropy of the ones for *lt*-SnO (at the *M* point of the BZ) is slightly larger. Comparison to experimental or other theoretical results is given in Refs. 44, 45, and 87.

From Table II it becomes clear that the electron masses for the different oxides decrease by almost a factor of two going along the row MgO, ZnO, SnO$_2$, In$_2$O$_3$, and CdO. Contrary, the values of the electron masses for SnO and SiO$_2$ are larger than for the other oxides. Again, we want to emphasize that the parabolic approximation is only fulfilled in the close vicinity around the Γ point. From our calculations of the effective electron masses we conclude that the electron

mobilities should be large in rs-CdO, rh-In$_2$O$_3$, and rutile- (rt) SnO$_2$ with the ones of the other oxides being up to a factor of 2.7 smaller.

In addition, we used the electronic structures derived from the HSE+G_0W_0 approach also for the derivation of the charge-neutrality levels and, hence, the band alignment for different materials.[45,89–91] Furthermore, the HSE+G_0W_0 approach has successfully been applied to describe nitride systems,[39,92–95] anti-ferromagnetic transition-metal oxides,[41,75] biaxially and uniaxially strained ZnO,[45,64] and the non-equilibrium wz polymorphs of MgO and CdO.[45,62]

IV. OPTICAL ABSORPTION

The optical absorption coefficients calculated from the solution of the BSE for rs-MgO, wz-ZnO, rs-CdO, rt-SnO$_2$, and lt-SnO are depicted in Fig. 2. We found that the inclusion of excitonic effects in the description is critically important for the TCOs as they (i) dominate the spectral features around the absorption onset,[43–45,61,64] and (ii) strongly influence the overall spectral shape.[43,45]

As a consequence, a pronounced excitonic peak is visible around the absorption onset, in particular, of rs-MgO and rt-SnO$_2$ [see Fig. 2(a) and (d)]. Such a peak also occurs at the onset of the absorption for wz-ZnO even though this is not as obvious from Fig. 2(b) due to the scale of this plot. Contrary, the influence of such an excitonic bound state is significantly smaller for rs-CdO and lt-SnO [cf. Fig. 2(c) and (e)]. One reason is that these two materials have indirect fundamental band gaps and, in addition, the electronic dielectric screening is significantly stronger for these two semiconductors which is why the excitonic effects are reduced.

The influence of the electron-hole interaction on the overall line shape is referred to as redistribution of oscillator strength in the literature. For all the oxides, peaks at higher photon energies are red-shifted due to the excitonic effects by about $1 \ldots 2$ eV.[43–45] In addition, a strong enhancement of the peak intensities and plateau heights due to the Coulomb interaction occurs at low photon energies.

Comparing the dielectric functions calculated from the solution of the BSE to experimental results has shown a very good agreement, for instance, for MgO, ZnO, and CdO,[43,45] but also for SnO$_2$.[44] Peak positions and relative peak heights are very well described by the calculations for these materials. We want to point out that the scissors operator Δ, that is used to mimic the QP gaps, does not reproduce the energy dependence of the self-energy operator Σ. Hence, we

find a general trend of a slight underestimation of the energy positions of the higher-lying CBs.[45] In addition, the absolute value of the absorption coefficient turns out to be underestimated in the calculations (e.g. for ZnO[50]), which can be explained, for instance, by imperfect samples, whereas our calculations describe defect-free crystals.

By linearly extrapolating the slope of the absorption curves (cf. Fig. 2) around the half maximum of the onset to zero absorption, we obtained the optical gaps of the oxides compiled in Table II. We want to point out the strong (noticeable) optical anisotropy of lt-SnO and rt-SnO$_2$ (wz-ZnO). In the case of rs-MgO and wz-ZnO the optical gaps are significantly smaller than the QP gaps also given in Table II. For these two materials this difference arises mostly due to the binding energies of the lowest bound excitonic states[45,64,80] that reduces the optical gaps with respect to the QP gaps. In addition, the Lorentzian broadening of 0.1 eV, which is used to account for temperature, instrumental, and lifetime effects, further leads to a reduction of the optical band gap in our calculations. Both the broadening effect as well as the exciton binding energy also play a role for rt-SnO$_2$. However, as elucidated in Ref. 44, the optical transitions between the uppermost valence-band and the lowest conduction-band states are dipole forbidden in this material; consequently, the optical gap is found to be much larger than the QP band gap (cf. Table II).

In the case of rs-CdO and lt-SnO the optical gap is found to be in between the lowest indirect and the lowest direct QP gap. For these two materials the dielectric screening is much larger which is the reason why there occurs no pronounced peak due to a bound excitonic state at the absorption onset. Nevertheless, excitonic effects are responsible for the optical gap being smaller than the lowest indirect gap for CdO, in addition to the broadening (see above). In the case of lt-SnO, the LDA+U+Δ description of the uppermost valence band at the M point of the BZ differs by 0.73 eV from the HSE+G_0W_0 result. This explains why the optical band gap found in our calculations turns out to be underestimated by this amount; also an influence on the line shape of the spectrum cannot be excluded and will be further investigated in the future.

The results for the dielectric functions obtained from the solution of the BSE have also been used to compute reflectivities as well as the electron-energy loss functions for MgO, ZnO, and CdO.[43,45] For these materials we identified valence and conduction-band levels (as well as their atomic origin) that are involved in the transitions that cause the main peaks of the spectra. The lowest eigenstates of the excitonic Hamiltonian have been calculated for MgO[80] as well as (strained and unstrained) ZnO.[64] In the case of AlN and CaO the BSE approach helped to identify the importance of van Hove singularities and of the excitonic effects for the absorption spectra.[96]

V. SUMMARY

In this paper the quasiparticle band structures of MgO, ZnO, CdO, SnO_2, SnO, In_2O_3, and SiO_2, calculated using the HSE+G_0W_0 approach, have been presented. For these different oxides we conclude that our results agree well with experimental findings, regarding, for instance, fundamental band gaps and band dispersions or effective electron masses. In addition, we presented the optical absorption spectra of MgO, ZnO, CdO, SnO_2, and SnO. We showed that for these oxides the impact of excitonic effects is significant and has to be taken into account in the calculations. We find that this task can be successfully accomplished by solving the Bethe-Salpeter equation. For SnO we conclude that the LDA+U+Δ approach does not reproduce the HSE+G_0W_0 results well enough, hence, a reliable parameter-free description of the optical properties requires future effort.

[*] a.schleife@llnl.gov

[1] David S. Ginley and Clark Bright, "Transparent conducting oxides," MRS Bull. **25**, 15–18 (2000).

[2] Elvira Fortunato, David Ginley, Hideo Hosono, and David C. Paine, "Transparent conducting oxides for photovoltaics," MRS Bull. **32**, 242–247 (2007).

[3] A. Schleife, C. Rödl, J. Furthmüller, and F. Bechstedt, "Electronic and optical properties of $Mg_xZn_{1-x}O$ and $Cd_x Zn_{1-x}O$ from ab initio calculations," New J. Phys. **13**, 085012 (2011).

[4] Atsuto Seko, Atsushi Togo, Fumiyasu Oba, and Isao Tanaka, "Structure and stability of a homologous series of tin oxides," Phys. Rev. Lett. **100**, 045702 (2008).

[5] Stephan Lany and Alex Zunger, "Dopability, intrinsic conductivity, and nonstoichiometry of transparent conducting oxides," Phys. Rev. Lett. **98**, 045501 (2007).

[6] B. E. Sernelius, K.-F. Berggren, Z.-C. Jin, I. Hamberg, and C. G. Granqvist, "Band-gap tailoring of ZnO by means of heavy Al doping," Phys. Rev. B **37**, 10244–10248 (1988).

[7] Radhouane Bel Hadj Tahar, Takayuki Ban, Yutaka Ohya, and Yasutaka Takahashi, "Tin doped indium oxide thin films: Electrical properties," J. Appl. Phys. **83**, 2631–2645 (1998).

[8] Z. Q. Li, Y. L. Yin, X. D. Liu, L. Y. Li, H. Liu, and Q. G. Song, "Electronic structure and optical properties of Sb-doped SnO_2," J. Appl. Phys. **106**, 083701 (2009).

[9] M. E. White, O. Bierwagen, M. Y. Tsai, and J. S. Speck, "Electron transport properties of antimony doped SnO_2 single crystalline thin films grown by plasma-assisted molecular beam epitaxy," J. Appl. Phys. **106**, 093704 (2009).

[10] D. Bruce Buchholz, Jun Liu, Tobin J. Marks, Ming Zhang, and Robert P. H. Chang, "Control and characterization of the structural, electrical, and optical properties of amorphous Zinc-Indium-Tin oxide thin films," ACS Applied Materials & Interfaces **1**, 2147–2153 (2009).

[11] Tadatsugu Minami, "Transparent conducting oxide semiconductors for transparent electrodes," Semicond. Sci. Tech. **20**, S35 (2005).

[12] Jia Sun, Aixia Lu, Liping Wang, Yu Hu, and Qing Wan, "High-mobility transparent thin-film transistors with an Sb-doped SnO_2 nanocrystal channel fabricated at room temperature," Nanotechnology **20**, 335204 (2009).

[13] Oliver Bierwagen and James S. Speck, "High electron mobility In_2O_3(001) and (111) thin films with nondegenerate electron concentration," Appl. Phys. Lett. **97**, 072103 (2010).

[14] W. A. Badawy, "Improvement of n-Si/SnO_2 electrolyte photoelectrochemical cells by Ru deposits," J. Electroanal. Chem. **281**, 85–95 (1990).

[15] Richard R. Lunt and Vladimir Bulovic, "Transparent, near-infrared organic photovoltaic solar cells for window and energy-scavenging applications," Appl. Phys. Lett. **98**, 113305 (2011).

[16] Andreas Klein, Christoph Körber, André Wachau, Frank Säuberlich, Yvonne Gassenbauer, Steven P. Harvey, Diana E. Proffit, and Thomas O. Mason, "Transparent conducting oxides for photovoltaics: Ma-

nipulation of Fermi level, work function and energy band alignment," Materials **3**, 4892–4914 (2010).

[17] John Robertson, "High dielectric constant gate oxides for metal oxide Si transistors," Rep. Prog. Phys. **69**, 327 (2006).

[18] Karla R. Reyes-Gil, Enrique A. Reyes-Garca, and Daniel Raftery, "Nitrogen-doped In_2O_3 thin film electrodes for photocatalytic water splitting," J. Phys. Chem. C **111**, 14579–14588 (2007).

[19] T. Nagata, O. Bierwagen, M. E. White, M. Y. Tsai, Y. Yamashita, H. Yoshikawa, N. Ohashi, K. Kobayashi, T. Chikyow, and J. S. Speck, "XPS study of Sb-/In-doping and surface pinning effects on the Fermi level in SnO_2 (101) thin films," Appl. Phys. Lett. **98**, 232107 (2011).

[20] L. F. J. Piper, Leyla Colakerol, P. D. C. King, A. Schleife, J. Zúñiga-Pérez, Per-Anders Glans, Tim Learmonth, A. Federov, T. D. Veal, F. Fuchs, V. Muñoz-Sanjosé, F. Bechstedt, C. F. McConville, and Kevin E. Smith, "Observation of quantized subband states and evidence for surface electron accumulation in CdO from angle-resolved photoemission spectroscopy," Phys. Rev. B **78**, 165127 (2008).

[21] M. W. Allen, C. H. Swartz, T. H. Myers, T. D. Veal, C. F. McConville, and S. M. Durbin, "Bulk transport measurements in ZnO: The effect of surface electron layers," Phys. Rev. B **81**, 075211 (2010).

[22] Oliver Bierwagen, James S. Speck, Takahiro Nagata, Toyohiro Chikyow, Yoshiyuki Yamashita, Hideki Yoshikawa, and Keisuke Kobayashi, "Depletion of the In_2O_3(001) and (111) surface electron accumulation by an oxygen plasma surface treatment," Appl. Phys. Lett. **98**, 172101 (2011).

[23] M. W. Allen, D. Y. Zemlyanov, G. I. N. Waterhouse, J. B. Metson, T. D. Veal, C. F. McConville, and S. M. Durbin, "Polarity effects in the x-ray photoemission of ZnO and other wurtzite semiconductors," Appl. Phys. Lett. **98**, 101906 (2011).

[24] Sebastian Küfner, *Ab-initio Untersuchung von Zinnmonoxid- und Zinndioxidoberflächen*, Master's thesis, Friedrich-Schiller-University Jena (2011).

[25] Péter Ágoston and Karsten Albe, "Thermodynamic stability, stoichiometry, and electronic structure of bcc-In_2O_3 surfaces," Phys. Rev. B **84**, 045311 (2011).

[26] Xiang Yang Kong and Zhong Lin Wang, "Structures of indium oxide nanobelts," Solid State Commun. **128**, 1–4 (2003).

[27] Y. Li, Y. Bando, and D. Golberg, "Single-crystalline In_2O_3 nanotubes filled with In," Adv. Mater. **15**, 581–585 (2003).

[28] A. Beltrán, J. Andrés, E. Longo, and E. R. Leite, "Thermodynamic argument about SnO_2 nanoribbon growth," Appl. Phys. Lett. **83**, 635–637 (2003).

[29] Jian Yu Huang, Li Zhong, Chong Min Wang, John P. Sullivan, Wu Xu, Li Qiang Zhang, Scott X. Mao, Nicholas S. Hudak, Xiao Hua Liu, Arunkumar Subramanian, Hongyou Fan, Liang Qi, Akihiro Kushima, and Ju Li, "In situ observation of the electrochemical lithiation of a single SnO_2 nanowire electrode," Science **330**, 1515–1520 (2010).

[30] Vesna Müller, Matthias Rasp, Goran Štefanić, Jianhua Ba, Sebastian Günther, Jiri Rathousky, Markus Niederberger, and Dina Fattakhova-Rohlfing, "Highly conducting nanosized monodispersed antimony-doped tin oxide particles synthesized via nonaqueous solgel procedure," Chem. Mater. **21**, 5229–5236 (2009).

[31] Markus R. Wagner, Jan-Hindrik Schulze, Ronny Kirste, Munise Cobet, Axel Hoffmann, Christian Rauch, Anna V. Rodina, Bruno K. Meyer, Uwe Röder, and Klaus Thonke, "Γ_7 valence band symmetry related hole fine splitting of bound excitons in ZnO observed in magneto-optical studies," Phys. Rev. B **80**, 205203 (2009).

[32] M. R. Wagner, G. Callsen, J. S. Reparaz, J.-H. Schulze, R. Kirste, M. Cobet, I. A. Ostapenko, S. Rodt, C. Nenstiel, M. Kaiser, A. Hoffmann, A. V. Rodina, M. R. Phillips, S. Lautenschläger, S. Eisermann, and B. K. Meyer, "Bound excitons in ZnO: Structural defect complexes versus shallow impurity centers," Phys. Rev. B **84**, 035313 (2011).

[33] F. Matino, L. Persano, V. Arima, D. Pisignano, R. I. R. Blyth, R. Cingolani, and Ross Rinaldi, "Electronic structure of indium-tin-oxide films fabricated by reactive electron-beam deposition," Phys. Rev. B **72**, 085437 (2005).

[34] Ch. Y. Wang, V. Cimalla, H. Romanus, Th. Kups, G. Ecke, Th. Stauden, M. Ali, V. Lebedev, J. Pezoldt, and O. Ambacher, "Phase selective growth and properties of rhombohedral and cubic indium oxide," Appl. Phys. Lett. **89**, 011904 (2006).

[35] Walter R. L. Lambrecht, Anna V. Rodina, Sukit Limpijumnong, B. Segall, and Bruno K. Meyer, "Valence-band ordering and magneto-optic exciton fine structure in ZnO," Phys. Rev. B **65**, 075207 (2002).

[36] J. Robertson, "Electronic structure of SnO_2, GeO_2, PbO_2, TeO_2 and MgF_2," J. Phys. C Solid State **12**, 4767 (1979).

[37] A. Svane and E. Antoncik, "Electronic structure of rutile SnO_2, GeO_2 and TeO_2," J. Phys. Chem. Solids **48**, 171–180 (1987).

[38] K. Reimann and M. Steube, "Experimental determination of the electronic band structure of SnO_2," Solid State Commun. **105**, 649–652 (1998).

[39] F. Fuchs, J. Furthmüller, F. Bechstedt, M. Shishkin, and G. Kresse, "Quasiparticle band structure based on a generalized Kohn-Sham scheme," Phys. Rev. B **76**, 115109 (2007).

[40] F. Bechstedt, F. Fuchs, and G. Kresse, "Ab-initio theory of semiconductor band structures: New developments and progress," Phys. Status Solidi B **246**, 1877–1892 (2009).

[41] C. Rödl, F. Fuchs, J. Furthmüller, and F. Bechstedt, "Ab initio theory of excitons and optical properties for spin-polarized systems: Application to antiferromagnetic MnO," Phys. Rev. B **77**, 184408 (2008).

[42] F. Bechstedt, F. Fuchs, and J. Furthmüller, "Spectral properties of InN and its native oxide from first principles," Phys. Status Solidi A **207**, 1041–1053 (2010).

[43] A. Schleife, C. Rödl, F. Fuchs, J. Furthmüller, and F. Bechstedt, "Optical and energy-loss spectra of MgO, ZnO, and CdO from ab initio many-body calculations," Phys. Rev. B **80**, 035112 (2009).

[44] A. Schleife, J. B. Varley, F. Fuchs, C. Rödl, F. Bechstedt, P. Rinke, A. Janotti, and C. G. Van de Walle, "Tin dioxide from first principles: Quasiparticle electronic states and optical properties," Phys. Rev. B **83**, 035116 (2011).

[45] André Schleife, *Exciting Imperfection: Real-structure effects in magnesium-, cadmium-, and zinc-oxide*, Phd thesis, Friedrich-Schiller-Universität, Jena (2010); *Electronic and optical properties of MgO, ZnO, and CdO* (Südwestdeutscher Verlag für Hochschulschriften, 2011).

[46] Qimin Yan, Patrick Rinke, M. Winkelnkemper, A. Qteish, D. Bimberg, Matthias Scheffler, and Chris G. Van de Walle, "Band parameters and strain effects in ZnO and group-III nitrides," Semicond. Sci. Tech. **26**, 014037 (2011).

[47] A. Schleife, M. Eisenacher, C. Rödl, F. Fuchs, J. Furthmüller, and F. Bechstedt, "Ab initio description of heterostructural alloys: Thermodynamic and structural properties of $Mg_xZn_{1-x}O$ and $Cd_xZn_{1-x}O$," Phys. Rev. B **81**, 245210 (2010).

[48] Patrick Rinke, André Schleife, Emmanouil Kioupakis, Andrea Marini, Anderson Janotti, Claudia Rödl, Friedhelm Bechstedt, Matthias Scheffler, and Chris G. Van de Walle, "First-principles optical spectra for F centers in MgO," Phys. Rev. Lett. (2012), in press.

[49] J. Furthmüller, F. Hachenberg, A. Schleife, D. Rogers, F. Hosseini Teherani, and F. Bechstedt, "Clustering of N impurities in ZnO," Appl. Phys. Lett. **100**, 022107 (2012).

[50] André Schleife, Claudia Rödl, Frank Fuchs, Karsten Hannewald, and Friedhelm Bechstedt, "Optical absorption in degenerately doped semiconductors: Mott transition or Mahan excitons?" Phys. Rev. Lett. **107**, 236405 (2011).

[51] Péter Ágoston, Karsten Albe, Risto M. Nieminen, and Martti J. Puska, "Intrinsic *n*-type behavior in transparent conducting oxides: A comparative hybrid-functional study of In_2O_3, SnO_2, and ZnO," Phys. Rev. Lett. **103**, 245501 (2009).

[52] Péter Ágoston, Christoph Körber, Andreas Klein, Martti J. Puska, Risto M. Nieminen, and Karsten Albe, "Limits for *n*-type doping in In_2O_3 and SnO_2: A theoretical approach by first-principles calculations using hybrid-functional methodology," J. Appl. Phys. **108**, 053511 (2010).

[53] P. Hohenberg and W. Kohn, "Inhomogeneous electron gas," Phys. Rev. **136**, B864–B871 (1964).

[54] W. Kohn and L. J. Sham, "Self-consistent equations including exchange and correlation effects," Phys. Rev. **140**, A1133–A1138 (1965).

[55] Mark S. Hybertsen and Steven G. Louie, "Electron correlation in semiconductors and insulators: Band gaps and quasiparticle energies," Phys. Rev. B **34**, 5390–5413 (1986).

[56] Lars Hedin, "New method for calculating the one-particle Green's function with application to the electron-gas problem," Phys. Rev. **139**, A796–A823 (1965).

[57] Lars Hedin and Stig Lundqvist, "Effects of electron-electron and electron-phonon interactions on the one-electron states of solids," in *Advances in Research and Applications*, Solid State Physics, Vol. 23, edited by David Turnbull Frederick Seiz and Henry Ehrenreich (Academic Press, 1970) pp. 1–181.

[58] Jochen Heyd, Gustavo E. Scuseria, and Matthias Ernzerhof, "Erratum: "Hybrid functionals based on a screened coulomb potential" [J. Chem. Phys. **118**, 8207 (2003)]," J. Chem. Phys. **124**, 219906 (2006).

[59] J. Paier, M. Marsman, K. Hummer, G. Kresse, I. C. Gerber, and J. G. Ángyán, "Screened hybrid density functionals applied to solids," J. Chem. Phys. **124**, 154709 (2006).

[60] J. Paier, M. Marsman, K. Hummer, G. Kresse, I. C. Gerber, and J. G. Ángyán, "Erratum: "Screened hybrid density functionals applied to solids" [J. Chem. Phys. **124**, 154709 (2006)]," J. Chem. Phys. **125**, 249901 (2006).

[61] A. Schleife, C. Rödl, F. Fuchs, J. Furthmüller, F. Bechstedt, P. H. Jefferson, T. D. Veal, C. F. Mc-Conville, L. F. J. Piper, A. DeMasi, K. E. Smith, H. Lösch, R. Goldhahn, C. Cobet, J. Zúñiga-Pérez, and V. Muñoz-Sanjosé, "*Ab-initio* studies of electronic and spectroscopic properties of MgO, ZnO, and CdO," J. Korean Phys. Soc. **53**, 2811–2815 (2008).

[62] A. Schleife, F. Fuchs, C. Rödl, J. Furthmüller, and F. Bechstedt, "Band-structure and optical-transition parameters of wurtzite MgO, ZnO, and CdO from quasiparticle calculations," Phys. Status Solidi B **246**, 2150–2153 (2009).

[63] D. Hobbs, G. Kresse, and J. Hafner, "Fully unconstrained noncollinear magnetism within the projector augmented-wave method," Phys. Rev. B **62**, 11556–11570 (2000).

[64] A. Schleife, C. Rödl, F. Fuchs, J. Furthmüller, and F. Bechstedt, "Strain influence on valence-band ordering and excitons in ZnO: An ab initio study," Appl. Phys. Lett. **91**, 241915 (2007).

[65] Vladimir I. Anisimov, Jan Zaanen, and Ole K. Andersen, "Band theory and Mott insulators: Hubbard U instead of Stoner I," Phys. Rev. B **44**, 943–954 (1991).

[66] S. L. Dudarev, G. A. Botton, S. Y. Savrasov, C. J. Humphreys, and A. P. Sutton, "Electron-energy-loss spectra and the structural stability of nickel oxide: An LSDA+U study," Phys. Rev. B **57**, 1505–1509 (1998).

[67] Wilfried G. Aulbur, Lars Jönsson, and John W. Wilkins, "Quasiparticle calculations in solids," in *Advances in Research and Applications*, Solid State Physics, Vol. 54, edited by Henry Ehrenreich and Frans Spaepen (Academic Press, 1999) pp. 1–218.

[68] G. Kresse and J. Furthmüller, "Efficient iterative schemes for ab initio total-energy calculations using a plane-wave basis set," Phys. Rev. B **54**, 11169–11186 (1996).

[69] G. Kresse and J. Furthmüller, "Efficiency of ab-initio total energy calculations for metals and semiconductors using a plane-wave basis set," Comp. Mater. Sci. **6**, 15–50 (1996).

[70] M. Shishkin and G. Kresse, "Implementation and performance of the frequency-dependent GW method within the PAW framework," Phys. Rev. B **74**, 035101 (2006).

[71] P. E. Blöchl, "Projector augmented-wave method," Phys. Rev. B **50**, 17953–17979 (1994).

[72] G. Kresse and D. Joubert, "From ultrasoft pseudopotentials to the projector augmented-wave method," Phys. Rev. B **59**, 1758–1775 (1999).

[73] G. Strinati, "Application of the Green's functions method to the study of the optical properties of semiconductors," Riv. Nuovo Cimento **11**, 1–86 (1988).

[74] Giovanni Onida, Lucia Reining, and Angel Rubio, "Electronic excitations: density-functional versus many-body Green's-function approaches," Rev. Mod. Phys. **74**, 601–659 (2002).

[75] C. Rödl, F. Fuchs, J. Furthmüller, and F. Bechstedt, "Quasiparticle band structures of the antiferromagnetic transition-metal oxides MnO, FeO, CoO, and NiO," Phys. Rev. B **79**, 235114 (2009).

[76] M. Gajdoš, K. Hummer, G. Kresse, J. Furthmüller, and F. Bechstedt, "Linear optical properties in the projector-augmented wave methodology," Phys. Rev. B **73**, 045112 (2006).

[77] Stefan Albrecht, Lucia Reining, Rodolfo Del Sole, and Giovanni Onida, "Ab initio calculation of excitonic effects in the optical spectra of semiconductors," Phys. Rev. Lett. **80**, 4510–4513 (1998).

[78] Lorin X. Benedict, Eric L. Shirley, and Robert B. Bohn, "Optical absorption of insulators and the electron-hole interaction: An ab initio calculation," Phys. Rev. Lett. **80**, 4514–4517 (1998).

[79] Michael Rohlfing and Steven G. Louie, "Electron-hole excitations in semiconductors and insulators," Phys. Rev. Lett. **81**, 2312–2315 (1998).

[80] F. Fuchs, C. Rödl, A. Schleife, and F. Bechstedt, "Efficient $\mathcal{O}(N^2)$ approach to solve the Bethe-Salpeter equation for excitonic bound states," Phys. Rev. B **78**, 085103 (2008).

[81] W. G. Schmidt, S. Glutsch, P. H. Hahn, and F. Bechstedt, "Efficient $\mathcal{O}(N^2)$ method to solve the Bethe-Salpeter equation," Phys. Rev. B **67**, 085307 (2003).

[82] R. de L. Kronig, "On the theory of dispersion of x-rays," J. Opt. Soc. Am. **12**, 547–556 (1926); H. A. Kramers, Nature **117**, 775 (1926).

[83] Wan-Jian Yin, Su-Huai Wei, Mowafak M. Al-Jassim, and Yanfa Yan, "Prediction of the chemical trends of oxygen vacancy levels in binary metal oxides," Appl. Phys. Lett. **99**, 142109 (2011).

[84] P. D. C. King, T. D. Veal, A. Schleife, J. Zúñiga-Pérez, B. Martel, P. H. Jefferson, F. Fuchs, V. Muñoz-Sanjosé, F. Bechstedt, and C. F. McConville, "Valence-band electronic structure of CdO, ZnO, and MgO from x-ray photoemission spectroscopy and quasi-particle-corrected density-functional theory calculations," Phys. Rev. B **79**, 205205 (2009).

[85] L. F. J. Piper, Alex DeMasi, Kevin E. Smith, A. Schleife, F. Fuchs, F. Bechstedt, J. Zúñiga-Pérez, and V. Muñoz-Sanjosé, "Electronic structure of single-crystal rocksalt CdO studied by soft x-ray spectroscopies and ab initio calculations," Phys. Rev. B **77**, 125204 (2008).

[86] A. R. H. Preston, B. J. Ruck, L. F. J. Piper, A. DeMasi, K. E. Smith, A. Schleife, F. Fuchs, F. Bechstedt, J. Chai, and S. M. Durbin, "Band structure of ZnO from resonant x-ray emission spectroscopy," Phys. Rev. B **78**, 155114 (2008).

[87] F. Fuchs and F. Bechstedt, "Indium-oxide polymorphs from first principles: Quasiparticle electronic states," Phys. Rev. B **77**, 155107 (2008).

[88] A. Schleife, F. Fuchs, J. Furthmüller, and F. Bechstedt, "First-principles study of ground- and excited-state properties of MgO, ZnO, and CdO polymorphs," Phys. Rev. B **73**, 245212 (2006).

[89] A. Schleife, F. Fuchs, C. Rödl, J. Furthmüller, and F. Bechstedt, "Branch-point energies and band discontinuities of III-nitrides and III-/II-oxides from quasiparticle band-structure calculations," Appl. Phys. Lett. **94**, 012104 (2009).

[90] B. Höffling, A. Schleife, F. Fuchs, C. Rödl, and F. Bechstedt, "Band lineup between silicon and transparent conducting oxides," Appl. Phys. Lett. **97**, 032116 (2010).

[91] B. Höffling, A. Schleife, C. Rödl, and F. Bechstedt, "Band discontinuities at Si-TCO interfaces from quasiparticle calculations: Comparison of two alignment approaches," Phys. Rev. B **85**, 035305 (2012).

[92] A. Belabbes, L. C. de Carvalho, A. Schleife, and F. Bechstedt, "Cubic inclusions in hexagonal AlN, GaN, and InN: Electronic states," Phys. Rev. B **84**, 125108 (2011).

[93] Luiz Cláudio de Carvalho, André Schleife, and Friedhelm Bechstedt, "Influence of exchange and correlation on structural and electronic properties of AlN, GaN, and InN polytypes," Phys. Rev. B **84**, 195105 (2011).

[94] Luiz Cláudio de Carvalho, André Schleife, Frank Fuchs, and Friedhelm Bechstedt, "Valence-band splittings in cubic and hexagonal AlN, GaN, and InN," Appl. Phys. Lett. **97**, 232101 (2010).

[95] Emmanouil Kioupakis, Patrick Rinke, André Schleife, Friedhelm Bechstedt, and Chris G. Van de Walle, "Free-carrier absorption in nitrides from first principles," Phys. Rev. B **81**, 241201 (2010).

[96] A. Riefer, F. Fuchs, C. Rödl, A. Schleife, F. Bechstedt, and R. Goldhahn, "Interplay of excitonic effects and van Hove singularities in optical spectra: CaO and AlN polymorphs," Phys. Rev. B **84**, 075218 (2011).

[97] Sebastian Küfner, André Schleife, and Friedhelm Bechstedt, (2012), unpublished.

[98] Frank Fuchs, (2011), private communication.

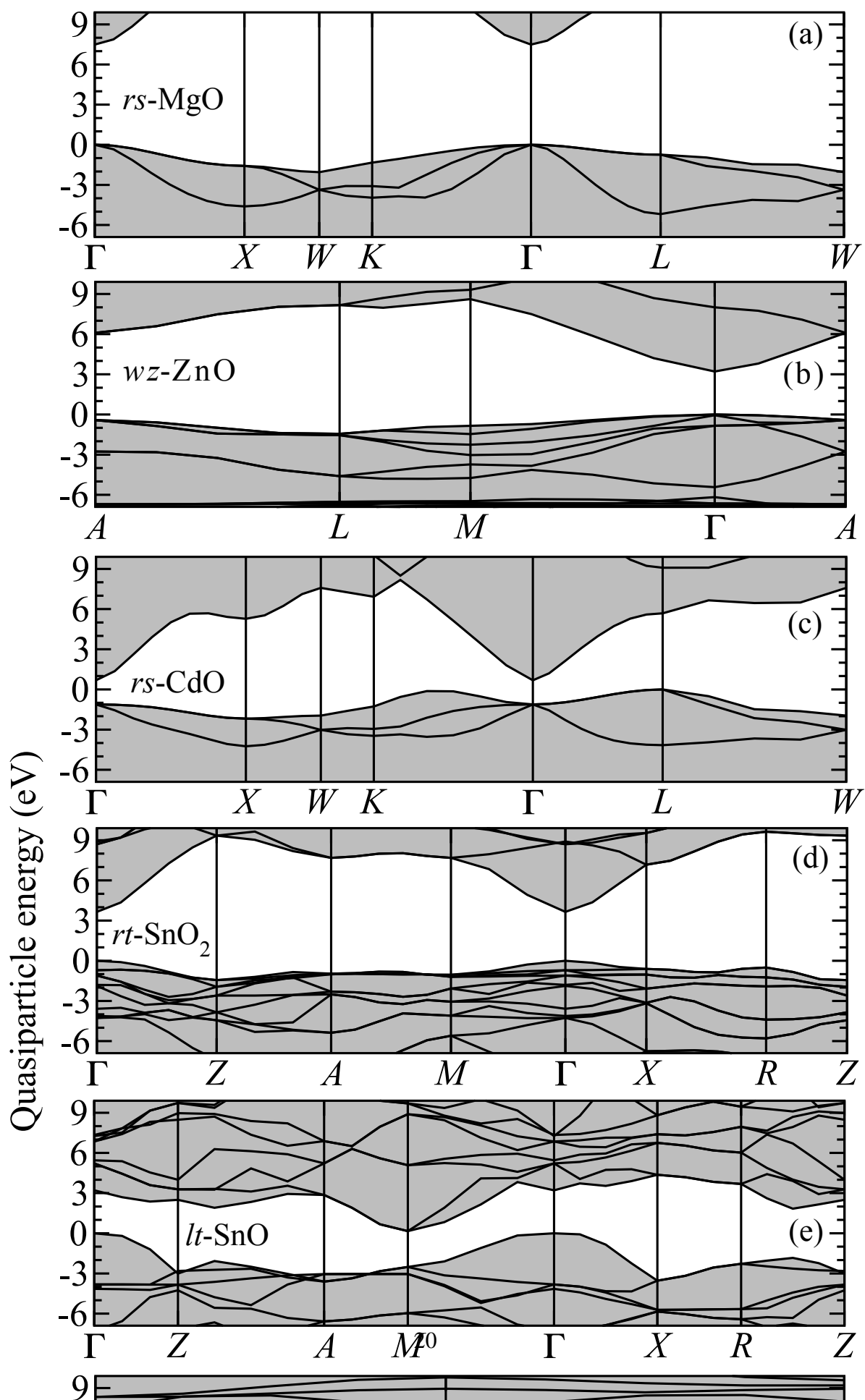**FIGURES**

Quasiparticle energy (eV)

FIG. 1. Quasiparticle band structures in the vicinity of the fundamental gap of (a) MgO, (b) ZnO, (c) CdO, (d) SnO_2, (e) SnO, (f) In_2O_3, and (g) SiO_2 calculated using the HSE+G_0W_0 approach. The valence-band maximum has been set to zero energy.
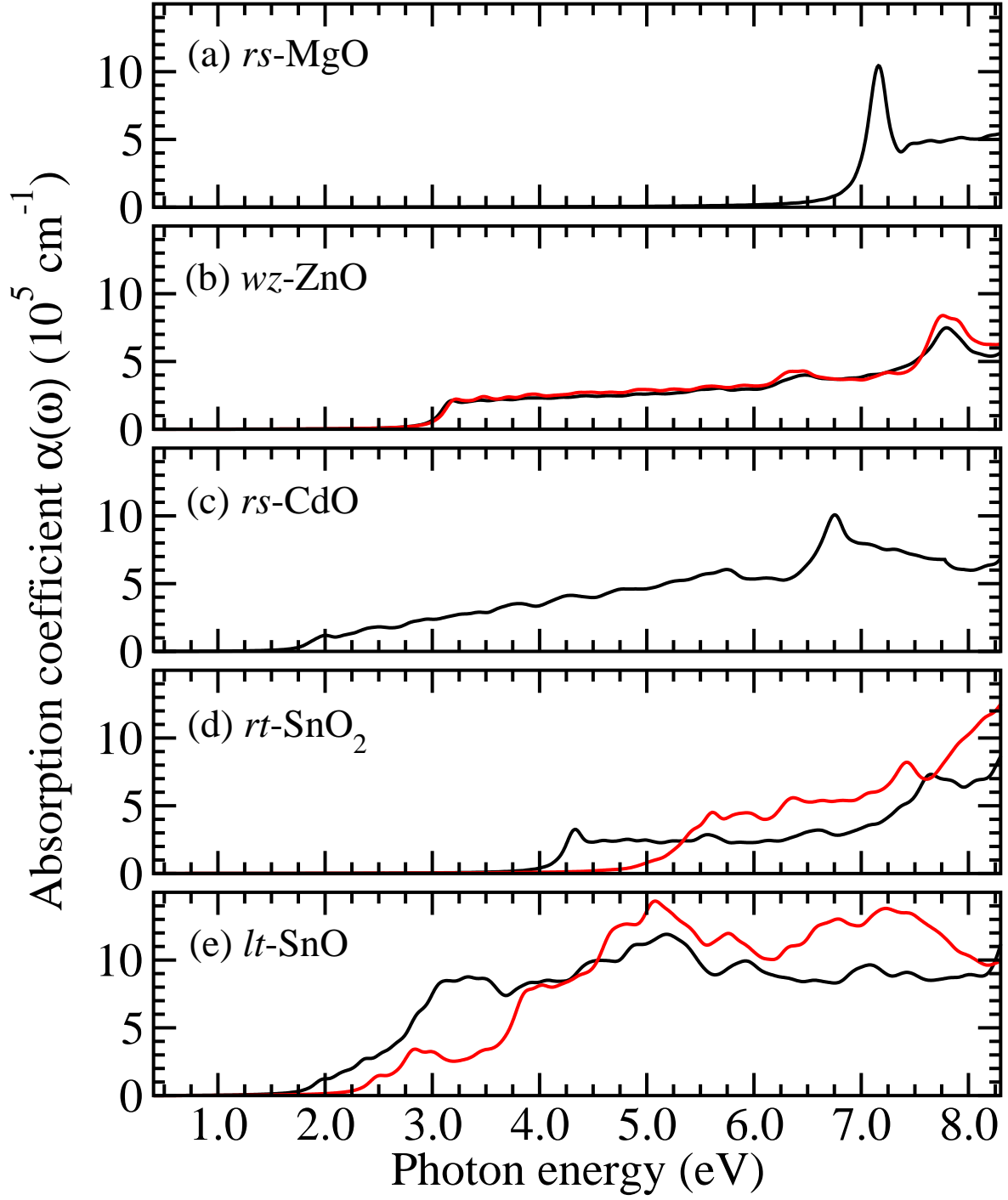
FIG. 2. (Color online) Absorption coefficient (in 10^5 cm^{-1}) around the fundamental band gap for different oxide semiconductors as calculated from the solution of the Bethe-Salpeter equation. Black (red) curves represent ordinary (extraordinary) light polarization.

TABLES

material	ground state	excited state
MgO, ZnO, CdO	Refs. 45 and 88	Refs. 43 and 45
SnO_2	Ref. 44	Ref. 44
SnO	Refs. 24 and 97	Refs. 24 and 97
In_2O_3	Ref. 87	Ref. 87
$Mg_xZn_{1-x}O$, $Cd_xZn_{1-x}O$	Refs. 45 and 47	Refs. 3 and 45
SiO_2	Ref. 98	Refs. 91 and 98

TABLE I. For each material the references are given that contain more information on the calculations of the ground-state and the excited-state properties that are reviewed in this work.

	$E_g^{dir}(\Gamma)$	E_g^{indir}	$E_g^{abs,\perp}$	$E_g^{abs,\|}$	m_e^*
rs-MgO	7.49	–	6.95	6.95	0.38
wz-ZnO	3.21	–	2.96	3.00	0.30
rs-CdO	1.81	0.68	1.73	1.73	0.21
rt-SnO$_2$	3.65	–	4.13	4.75	0.23
lt-SnO	3.21	0.16	1.79	2.29	0.42
rh-In$_2$O$_3$	3.25	–	–	–	0.22
β-SiO$_2$	8.76	–	–	–	0.57

TABLE II. Direct [$E_g^{dir}(\Gamma)$] and indirect (E_g^{indir}) QP band gaps as well as optical band gaps for ordinary ($E_g^{abs,\perp}$) and extraordinary ($E_g^{abs,\|}$) light polarization are given in eV. Harmonic mean values for the effective electron masses m_e^*, derived from the HSE+G_0W_0 band structure (HSE band structure for In$_2$O$_3$[87]), are given in units of the free-electron mass.

	rs-MgO	rs-CdO
$m^*_X(\Gamma^+_{6c})$	0.36	0.19
$m^*_K(\Gamma^+_{6c})$	0.42	0.25
$m^*_L(\Gamma^+_{6c})$	0.36	0.19
$m^*_X(\Gamma^-_{8v})$	1.85	4.85
$m^*_K(\Gamma^-_{8v})$	4.53	−1.35
$m^*_L(\Gamma^-_{8v})$	3.21	−1.98
$m^*_X(\Gamma^-_{8v})$	1.61	2.33
$m^*_K(\Gamma^-_{8v})$	1.65	3.52
$m^*_L(\Gamma^-_{8v})$	2.37	−3.63
$m^*_X(\Gamma^-_{6v})$	0.44	0.36
$m^*_K(\Gamma^-_{6v})$	0.44	0.38
$m^*_L(\Gamma^-_{6v})$	0.36	0.24

TABLE III. Effective masses m^* (in units of the free-electron mass m) at the BZ center along the $\Gamma-X$, $\Gamma-K$, and $\Gamma-L$ directions for rs-MgO and rs-CdO. Values are given for the lowest conduction band and the uppermost valence bands.